

1 **EMPIRICAL CORRELATIONS - DRAINED SHEAR STRENGTH**
2 **FOR SLOPE STABILITY ANALYSES**

3
4
5
6 Timothy D. Stark, F.ASCE, D.GE, Ph.D., P.E.
7 Professor of Civil and Environmental Engineering
8 University of Illinois at Urbana-Champaign
9 205 N. Mathews Ave.
10 Urbana, IL 61801
11 (217) 333-7394
12 (217) 333-9464 Fax
13 tstark@illinois.edu
14

15
16 *and*

17
18
19 Manzoor Hussain
20 Ph.D. (Civil Engineering)
21 College of Civil Engineering, Risalpur
22 National University of Sciences and Technology
23 Risalpur, Pakistan
24 mhussain@mce.nust.edu.pk
25
26
27
28

29 **Paper# GTENG-2476 – Revision#2**

30 A paper accepted for publication in the
31 *ASCE Journal of Geotechnical and Geoenvironmental Engineering*

32
33
34
35 August 14, 2012

36
37
38
39
40
41
42
43
44
45
46
47
48
49
50
51
52
53
54
55
56
57
58
59
60
61
62
63
64
65
66
67
68
69
70

EMPIRICAL CORRELATIONS - DRAINED SHEAR STRENGTH FOR SLOPE STABILITY ANALYSES

Timothy D. Stark, F.ASCE, D.GE and Manzoor Hussain

ABSTRACT: Empirical correlations provide estimates of parameter values for preliminary design, verification of laboratory shear test data, and confirmation of back-analysis of a failed slope. The empirical correlations presented herein use liquid limit, clay-size fraction, and effective normal stress to capture the variability and stress dependent nature of drained residual and fully softened strength envelopes. This paper describes the testing and analysis used to increase the number of data points in the existing correlations, expand the residual strength correlation to include an effective normal stress of 50 kPa, and develop correlations between values of liquid limit and clay-size fraction measured using sample processed through a Number 40 sieve (ASTM procedure) material and values derived using ball milled/disaggregated sample. In addition, equations are presented to express the empirical correlations which were used to develop a spreadsheet that estimates the residual and fully softened friction angles based on entered values of liquid limit and clay-size fraction.

Keywords: shear strength, residual friction angle, fully softened friction angle, empirical correlation, clay, shale

71
72
73
74
75
76
77
78
79
80
81
82
83
84
85
86
87
88
89
90
91
92
93
94
95
96
97
98
99

INTRODUCTION

Different empirical correlations, e.g., Skempton (1964), Lupini et al. (1981), Mitchell (1993), and Terzaghi et al. (1996), for drained residual and fully softened shear strengths have been proposed by considering these strengths as a function of a single or combination of parameters such as, clay-size fraction (CF), plasticity index (PI), and liquid limit (LL). Residual shear strength is primarily dependent on mineral composition, which is related to plasticity and grain size characteristics. Fully softened strength corresponds to random arrangements of clay particles and is numerically equivalent to the drained peak strength of a normally consolidated specimen (Skempton, 1970). Therefore, particle size, shape, interlocking, and degree of orientation are important in estimating the fully softened shear strength of clays. Both residual and fully softened strengths are stress dependent (Chandler, 1977, Lupini et al., 1981, Stark and Eid, 1994 and 1997, Mesri and Shahien, 2003, and Stark et al., 2005). Therefore, an empirical correlation incorporating effective normal stress, LL, and CF, as suggested by Stark and Eid (1994 and 1997) and Stark et al. (2005), provides a good estimate of the friction angles. These empirical correlations were developed using torsional ring shear test results and verified using back-analysis of landslide case histories.

This paper describes the testing and analysis used to increase the number of data points in the correlations suggested by Stark and Eid (1994 and 1997) and Stark et al. (2005) and also the effect of sample preparation on LL, CF, effective stress residual secant friction angle (ϕ'_r), and fully softened friction angle (ϕ'_{fs}). Additional improvements in the empirical correlations for drained ϕ'_r and ϕ'_{fs} include expanding the residual strength correlation to include an effective normal stress of 50 kPa, developing mathematical equations for each trend line in the three CF groups and each effective normal stress, and providing recommendations for use in stability analyses. The resulting mathematical equations were used to develop a spreadsheet for estimating values of drained residual and fully softened friction angles.

A stress dependent strength envelope is recommended for analysis of slopes and back-analysis of landslides (Stark and Eid, 1994 and 1997) and exhibits maximum curvature or stress

102 dependency at low effective normal stresses, i.e., effective normal stresses of less than 100 kPa.
103 As a result, it is desirable for the estimated strength envelope to include an effective normal
104 stress of 50 kPa. To accomplish this, the empirical correlation for drained residual friction angle
105 suggested by Stark et al. (2005) is extended herein to include an effective normal stress of 50 kPa
106 with new data and a normal stress trend line for 50 kPa for all three CF groups was developed.

107
108

109 **EMPIRICAL CORRELATION FOR DRAINED RESIDUAL SECANT FRICTION** 110 **ANGLE OF FINEGRAINED SOILS**

111

112 Many researchers, e.g., Skempton (1964), Voight (1973), Kanji (1974), Seycek (1978), Lupini et
113 al. (1981), Skempton (1985), Mesri and Cepeda-Diaz (1986), Collotta et al. (1989), Stark and
114 Eid (1994 and 1997), Mesri and Shahien (2003), Wesley (2003), and Tiwari and Marui (2005),
115 have proposed empirical correlations for drained residual friction angles using CF, LL, and/or
116 plasticity index (PI) of clays or some other parameter based on CF, PI, Activity, or LL. Stark and
117 Eid (1994) present ring shear drained residual friction angles as a function of LL and incorporate
118 the effect of CF and effective normal stress in a single correlation. The empirical correlation was
119 developed using ring shear test results on thirty-two natural clay soils. Stark et al. (2005) refine
120 the ϕ'_r empirical correlation proposed by Stark and Eid (1994) by adding test results for an
121 additional thirty-four soils for a total of sixty-six natural soils. The empirical correlation
122 proposed by Stark and Eid (1994) and refined by Stark et al. (2005) reduced the scatter as
123 compared to other empirical correlations. The scatter for each CF group of Stark et al. (2005) and
124 the correlations presented herein is about 3-4 degrees.

125
126

127 **Updated Empirical Correlation for Drained Residual Secant Friction Angle**

128

129 The empirical correlation for ϕ'_r suggested by Stark et al. (2005) incorporates the three main
130 factors, clay mineralogy (LL), amount of clay mineral (CF), and effective normal stress (σ'_n), that
131 influence the residual strength which helps to explain reduction in scatter. The correct estimate
132 of values of LL and CF measured using disaggregated samples discussed below, can assist in
133 estimating a reliable value of ϕ'_r . Thus, the correlation suggested by Stark et al. (2005) has been

134 used to provide estimates of ϕ'_r for use in preliminary design, verification of data obtained from
135 laboratory tests, and confirmation of back-analysis of failed slopes.

136

137 The empirical correlation uses three different CF groups, i.e., $CF \leq 20\%$, $25\% \leq CF \leq$
138 45% , and $CF \geq 50\%$, to account for three different shearing behaviors, i.e., rolling, transitional,
139 and sliding, respectively, as suggested by Lupini et al. (1981) and Skempton (1985). Values of
140 LL and CF can be used to estimate ϕ'_r for various effective normal stresses to develop a stress
141 dependent residual strength envelope. This stress dependent strength envelope should be used
142 directly in stability analyses of preexisting landslides instead of a friction angle and/or cohesion
143 value. Because a stress dependent residual strength envelope has more curvature at low values of
144 σ'_n , data for $\sigma'_n < 100$ kPa were developed and added to the empirical correlation herein.

145

146

147 ***Inclusion of $\sigma'_n = 50$ kPa in Correlation for Drained Residual Secant Friction Angle***

148

149 The nonlinear residual strength envelope is most pronounced, i.e., has greatest curvature, at low
150 effective normal stresses, e.g., $\sigma'_n < 100$ kPa, and it becomes more linear at higher effective
151 normal stresses (see ring shear data in Fig. 1). Stark and Eid (1994) and Stark et al. (2005)
152 present a relationship between LL and ϕ'_r for values of σ'_n of 100, 400, and 700 kPa for three CF
153 groups. However, Stark and Eid (1994) and Stark et al. (2005) do not present any data and/or a
154 trend line for $\sigma'_n < 100$ kPa. To capture this nonlinearity, a trend line for $\sigma'_n = 50$ kPa was
155 developed for each CF group so a well-defined stress dependent residual strength envelope could
156 be estimated using residual secant friction angles for values of σ'_n of 0, 50, 100, 400, and 700
157 kPa.

158

159 During the present study, torsional ring shear data from Eid (1996), data generated by
160 Stark et al. (2005), and testing of seven additional soils herein following ASTM D 6467 (ASTM,
161 2010a) were used to develop the trend line for $\sigma'_n = 50$ kPa. This brings the total number of
162 natural soils used to create the correlation shown in Fig. 2 to seventy-three (73). The empirical
163 correlation in Fig. 2 can be used to estimate the ϕ'_r values for σ'_n of 0, 50, 100, 400, and 700 kPa
164 using CF and LL of a soil. The estimated ϕ'_r value for each value of σ'_n can be used to calculate

165 the residual shear stress (τ_r) which can be used to plot the drained residual strength envelope
 166 using the origin. The stress dependent strength envelope developed from the five values of σ'_n (0,
 167 50, 100, 400, and 700 kPa) can be used directly in the stability analysis of preexisting landslides
 168 or slopes that may undergo shear movement.

169
 170 In summary, the addition of data and a trend line for $\sigma'_n = 50$ kPa in the empirical
 171 correlation shown in Fig. 2 provides a better estimate of the complete stress dependent residual
 172 strength envelope than prior correlations for use in stability analyses (see Fig. 1).

173
 174

175 ***Equations for Updated Empirical Correlations for Drained Residual Secant Friction Angle***

176
 177 Use of the correlation between LL and ϕ'_r in Fig. 2 requires the user to have the figure available
 178 to obtain values of ϕ'_r for a given LL and CF. Having the empirical correlation available only in
 179 graphical form also made it difficult to incorporate the correlation in slope stability software and
 180 continuum methods. As a result, the present study developed a separate mathematical equation
 181 for each σ'_n trend line of the proposed correlation which can be used to estimate ϕ'_r using LL and
 182 the CF group. The value of CF determines the required equation to be used, so the LL value is
 183 the only input parameter used in the equation to estimate ϕ'_r for various values of σ'_n .

184

185 The mathematical expressions developed herein are in excellent agreement with the trend
 186 lines, not the data, suggested by Stark et al. (2005). The empirical correlation for ϕ'_r of CF Group
 187 #1 and for LL values ranging from 30% to less than 80% ($30\% \leq LL < 80\%$) are shown as
 188 Equations (1.1) to (1.4) below. The upper bound for LL is specified because no ring shear data
 189 are available outside of this LL range. The ring shear data along with the trend lines sketched by
 190 Stark et al. (2005) for CF Group #1 and the trend lines sketched from the newly developed
 191 Equations (1.1) to (1.4) are compared in Fig. 3. Fig. 3 shows excellent agreement between the
 192 trend lines suggested in Fig. 2 and Equations (1.1) to (1.4). Thus, a second degree polynomial
 193 can adequately represent the trend lines for CF Group #1 for all four effective normal stresses.

194

195
$$(\phi_r)_{\sigma'_n=50\text{kPa}} = 39.71 - 0.29(LL) + 6.63 \times 10^{-4}(LL)^2 \quad (1.1)$$

196
$$(\phi_r)_{\sigma_n=100\text{kPa}} = 39.41 - 0.298(\text{LL}) + 6.81 \times 10^{-4}(\text{LL})^2 \quad (1.2)$$

197
$$(\phi_r)_{\sigma_n=400\text{kPa}} = 40.24 - 0.375(\text{LL}) + 1.36 \times 10^{-3}(\text{LL})^2 \quad (1.3)$$

198
$$(\phi_r)_{\sigma_n=700\text{kPa}} = 40.34 - 0.412(\text{LL}) + 1.683 \times 10^{-3}(\text{LL})^2 \quad (1.4)$$

199
 200 Another set of equations was developed for the trend lines in CF Group #2
 201 ($25\% \leq \text{CF} \leq 45\%$) and LL values ranging from 30% to less than 130% ($30\% \leq \text{LL} < 130\%$) and
 202 are given below in Equations (2.1) to (2.4). Again the upper bound for LL is specified because
 203 ring shear data are available only for this specific LL range. A third degree polynomial was used
 204 to obtain agreement between the trend lines for CF Group #2 and the mathematical expressions
 205 for all four effective normal stresses.

206
 207
$$(\phi_r)_{\sigma_n=50\text{kPa}} = 31.4 - 6.79 \times 10^{-3}(\text{LL}) - 3.616 \times 10^{-3}(\text{LL})^2 + 1.864 \times 10^{-5}(\text{LL})^3 \quad (2.1)$$

208
$$(\phi_r)_{\sigma_n=100\text{kPa}} = 29.8 - 3.627 \times 10^{-4}(\text{LL}) - 3.584 \times 10^{-3}(\text{LL})^2 + 1.854 \times 10^{-5}(\text{LL})^3 \quad (2.2)$$

209
$$(\phi_r)_{\sigma_n=400\text{kPa}} = 28.4 - 5.622 \times 10^{-2}(\text{LL}) - 2.952 \times 10^{-3}(\text{LL})^2 + 1.721 \times 10^{-5}(\text{LL})^3 \quad (2.3)$$

210
$$(\phi_r)_{\sigma_n=700\text{kPa}} = 28.05 - 0.2083(\text{LL}) - 8.183 \times 10^{-4}(\text{LL})^2 + 9.372 \times 10^{-6}(\text{LL})^3 \quad (2.4)$$

211
 212 The trend lines in CF Group #3, i.e., $\text{CF} \geq 50\%$, are divided into two parts to ensure the
 213 mathematical expressions are in agreement with the trend lines in Fig. 2. Two equations are
 214 required to capture the complicated shape of the Group #3 trend lines. Fig. 2 shows that the left
 215 portion of each trend line, i.e., $\text{LL} < 120\%$, has significant curvature so it is represented by a
 216 polynomial expression. The right portion of the trend line, i.e., $\text{LL} \geq 120\%$, is represented by a
 217 linear relationship. This necessitated using separate equations for LL values ranging between
 218 40% and less than 120% and LL values ranging between 120% and 300%. The upper and lower
 219 bounds for LL values are specified because of the availability of ring shear test data in this range.

220
 221 As shown in Equations (3.1) to (4.4), a third degree polynomial represents the trend lines
 222 for CF Group #3 and for all four effective normal stresses and for $30\% \leq \text{LL} < 120\%$ and the

223 trend lines for CF Group #3 and $120\% \leq LL \leq 300\%$ can be represented using a linear
 224 relationship (straight line).

225
 226
$$(\phi_r)_{\sigma'_n=50\text{kPa}} = 33.5 - 0.31(LL) + 3.9 \times 10^{-4}(LL)^2 + 4.4 \times 10^{-6}(LL)^3 \quad (3.1)$$

227
$$(\phi_r)_{\sigma'_n=100\text{kPa}} = 30.7 - 0.2504(LL) - 4.2053 \times 10^{-4}(LL)^2 + 8.0479 \times 10^{-6}(LL)^3 \quad (3.2)$$

228
$$(\phi_r)_{\sigma'_n=400\text{kPa}} = 29.42 - 0.2621(LL) - 4.011 \times 10^{-4}(LL)^2 + 8.718 \times 10^{-6}(LL)^3 \quad (3.3)$$

229
$$(\phi_r)_{\sigma'_n=700\text{kPa}} = 27.7 - 0.3233(LL) + 2.896 \times 10^{-4}(LL)^2 + 7.1131 \times 10^{-6}(LL)^3 \quad (3.4)$$

230
$$(\phi_r)_{\sigma'_n=50\text{kPa}} = 12.03 - 0.0215(LL) \quad (4.1)$$

231
$$(\phi_r)_{\sigma'_n=100\text{kPa}} = 10.64 - 0.0183(LL) \quad (4.2)$$

232
$$(\phi_r)_{\sigma'_n=400\text{kPa}} = 8.32 - 0.0114(LL) \quad (4.3)$$

233
$$(\phi_r)_{\sigma'_n=700\text{kPa}} = 5.84 - 0.0049(LL) \quad (4.4)$$

234
 235

236 ***Drained Residual Strength Envelope***

237

238 The empirical correlation in Fig. 2 results in a cohesion intercept of zero for the drained
 239 residual strength envelope. By definition the residual strength condition results from the
 240 reorientation of platy clay particles parallel to the direction of shear, which results in increased
 241 face-to-face interaction of the particles (Skempton 1985). The resulting shear strength is low
 242 because it is difficult for the face-to-face particles to establish contact or bonding between them
 243 (Terzaghi et al. 1996). The establishment of a residual strength condition also results in increased
 244 water content at or near the preexisting failure surface (Skempton 1985). In summary, the
 245 particle contact and bonding that leads to a cohesion strength parameter greater than zero have
 246 been significantly reduced or removed by the shear displacement required to reach a residual
 247 strength condition. This results in only a frictional shear resistance that is represented by a
 248 residual friction angle and the effective normal stress acting on the shear surface. Because the

249 residual strength is controlled by the frictional resistance of face-to-face particles, the residual
250 strength is a function of clay mineralogy. As a result, it is recommended that a stress dependent
251 strength envelope be used to model the drained residual strength and the resulting strength
252 envelope should pass through the origin, i.e., the value of effective stress cohesion strength
253 parameter should be zero, in stability analyses involving a residual strength condition.
254 Alternatively, the stress dependent can be used directly in the stability analysis instead of a
255 friction angle and cohesion.

256
257

258 **EMPIRICAL CORRELATION FOR DRAINED FULLY SOFTENED SECANT** 259 **FRICITION ANGLE FOR FINE-GRAINED SOILS**

260

261 The history of comparing peak effective stress friction angle (ϕ') of normally clay soils with
262 plasticity index (PI) can be traced back to the late 1950's. For example, Bjerrum and Simons
263 (1960) present a relationship that relates ϕ' to plasticity index (PI) for normally consolidated
264 soils. Although empirical correlations between ϕ' and PI are presented by Kenney (1959), Holt
265 (1962), Brooker and Ireland (1965), Mitchell (1965), Bjerrum (1967) and Deere (1967), these
266 correlations have considerable scatter which is noted by Kanji (1974). Subsequently, Skempton
267 (1970) equated the fully softened shear strength of a soil, which corresponds to the random
268 arrangement of clay particles, to the peak strength of a normally consolidated soil.

269

270 Skempton (1970) concludes that full softening reduces clay strength to the “critical state”
271 strength so there is no further strength loss due to increase in water content and void ratio.
272 However, additional strength loss can occur due to shear displacement. Field observations
273 indicate that the fully softened strength can be mobilized around excavations in fissured clays
274 (Skempton, 1977) and in desiccated, cracked, and weathered compacted clay embankments, e.g.,
275 levees, where infiltration of water along cracks results in higher water contents and void ratios
276 (Wright et al., 2007). Softening around excavations is primarily due to stress relief that results in
277 opening of fissures and development of negative pore-water pressures (Terzaghi, 1936).
278 Softening in highway (Wright et al., 2007) and levee slopes is primarily due to cycles of

279 desiccation and weathering that allows infiltration that results in clay swelling, an increase in
280 moisture content, and a strength reduction.

281

282

283 **Updated Empirical Correlation for Drained Fully Softened Secant Friction Angle**

284

285 The empirical correlation for drained fully softened secant friction angle proposed by Stark and
286 Eid (1997) and revised by Stark et al. (2005) only requires LL and CF to estimate the drained
287 fully softened friction angle (ϕ'_{fs}). Thus, the fully softened strength correlation suggested by
288 Stark et al. (2005) provides a reliable estimates of ϕ'_{fs} for use in preliminary design, verification
289 of laboratory test results, and confirmation of back-analysis of first time slides.

290

291 The fully softened strength empirical correlation uses three different CF groups, i.e., CF
292 $\leq 20\%$, $25\% \leq CF \leq 45\%$, and $CF \geq 50\%$, which is similar to the residual strength correlation
293 and accounts for the effect of CF and σ'_n on ϕ'_{fs} values. Furthermore, the empirical correlation
294 uses values of LL and CF measured using disaggregated samples to make it similar to the
295 empirical correlation for drained residual secant friction angle shown in Fig. 2.

296

297 The present study suggests a separate mathematical expression for each trend line of the
298 correlation in Fig. 4 that can be used to estimate values of ϕ'_{fs} and a stress dependent strength
299 envelope using values of LL and CF measured using disaggregated samples.

300

301

302 **Equations for Updated Empirical Correlations for Drained Fully Softened Secant Friction** 303 **Angle**

304

305 Stark and Eid (1997) and Stark et al. (2005) present a relationship between LL and drained fully
306 softened secant friction angle in graphical form with separate trend lines for each effective
307 normal stress for three different CF groups. The present study considered each CF group
308 separately while developing an equation for each trend line for the three effective normal stresses
309 considered, i.e., 50, 100, and 400 kPa. The empirical correlation for fully softened secant friction
310 angle in Stark et al. (2005) and Fig. 4 already includes an effective normal stress of 50 kPa so

311 this trend line did not have to be added during this study but was an impetus for adding this
 312 effective normal stress to the residual strength correlation. Stark et al. (2005) adjusted the ring
 313 shear fully softened strength by adding 2.5 degrees to the measured values to make these
 314 comparable to the values obtained using a triaxial compression test and more importantly first-
 315 time landslides (Skempton, 1970). This adjustment was deemed necessary by Stark and Eid
 316 (1997) and Stark et al. (2005) because first-time landslides usually do not involve a horizontal
 317 failure surface as is present in the ring shear device. The failure surface in first-time slides is
 318 closer to the orientation of the failure surface in a triaxial compression test so the existing and
 319 new values of ϕ'_{fs} were increased by 2.5 degrees to reflect the triaxial mode of shear. New data
 320 for three natural soils tested herein has been added to the existing database with this adjustment
 321 of 2.5 degrees and the updated correlation is shown in Fig. 4.

322

323 A set of three equations was developed during the present study for the empirical
 324 correlation for drained fully softened secant friction angles of CF Group #1 and for LL values
 325 ranging from 30% to less than 80% ($30\% \leq LL < 80\%$). These equations are given below as
 326 Equations (5.1) to (5.3). The LL range of 30 to 80% is specified because the ring shear data are
 327 available only for this LL range. A second degree polynomial can be used to represent the trend
 328 lines for CF Group #1 and for all three effective normal stresses.

329

$$330 \quad (\phi_r)_{\sigma'_n=50\text{kPa}} = 34.85 - 0.0709(LL) + 2.35 \times 10^{-4}(LL)^2 \quad (5.1)$$

$$331 \quad (\phi_r)_{\sigma'_n=100\text{kPa}} = 34.39 - 0.0863(LL) + 2.66 \times 10^{-4}(LL)^2 \quad (5.2)$$

$$332 \quad (\phi_r)_{\sigma'_n=400\text{kPa}} = 34.76 - 0.13(LL) + 4.71 \times 10^{-4}(LL)^2 \quad (5.3)$$

333

334 A set of three equations was also developed herein for CF Group #2 and LL values
 335 ranging from 30% to 130% ($30\% \leq LL \leq 130\%$) and is given below as Equations (6.1) to (6.3).
 336 A second degree polynomial was also used to represent the trend lines for CF Group #2 and for
 337 all three effective normal stresses.

338

$$339 \quad (\phi_r)_{\sigma'_n=50\text{kPa}} = 36.18 - 0.1143(LL) - 2.354 \times 10^{-4}(LL)^2 \quad (6.1)$$

340
$$(\phi_r)_{\sigma'_n=100\text{kPa}} = 33.11 - 0.107(\text{LL}) + 2.2 \times 10^{-4}(\text{LL})^2 \quad (6.2)$$

341
$$(\phi_r)_{\sigma'_n=400\text{kPa}} = 30.7 - 0.1263(\text{LL}) + 3.442 \times 10^{-4}(\text{LL})^2 \quad (6.3)$$

342

343 Another set of three equations was developed for CF Group #3 and LL values ranging
 344 from 30% to 300% ($30\% \leq \text{LL} \leq 300\%$) and is given below as Equations (7.1) to (7.3). A third
 345 degree polynomial also can be used to represent the trend lines for CF Group #3 and for all three
 346 effective normal stresses. The ring shear data along with the trend lines sketched by Stark et al.
 347 (2005) for CF Group #3, and the trend lines sketched from the newly developed Equations (7.1)
 348 to (7.3) are plotted on Fig. 5. Fig. 5 shows that the trend lines plotted using Equations (7.1) to
 349 (7.3) are in agreement with the trend lines suggested by Stark et al. (2005).

350

351
$$(\phi_r)_{\sigma'_n=50\text{kPa}} = 33.37 - 0.11(\text{LL}) + 2.344 \times 10^{-4}(\text{LL})^2 - 2.96 \times 10^{-7}(\text{LL})^3 \quad (7.1)$$

352
$$(\phi_r)_{\sigma'_n=100\text{kPa}} = 31.17 - 0.142(\text{LL}) + 4.678 \times 10^{-4}(\text{LL})^2 - 6.762 \times 10^{-7}(\text{LL})^3 \quad (7.2)$$

353
$$(\phi_r)_{\sigma'_n=400\text{kPa}} = 28.0 - 0.1533(\text{LL}) + 5.64 \times 10^{-4}(\text{LL})^2 - 8.414 \times 10^{-7}(\text{LL})^3 \quad (7.3)$$

354

355

356 ***Drained Fully Softened Strength Envelope***

357

358 Determining whether the value of effective stress cohesion should be equal to zero is a
 359 little more complicated for the fully softened condition than the residual strength condition.
 360 Skempton (1977) concludes that overconsolidated clays undergo a softening process that results
 361 in the fully softened strength being mobilized, not the shear strength of the intact or unsoftened
 362 overconsolidated clay, in slopes that have not undergone previous sliding (first-time slides). This
 363 softening process reduces the effective stress cohesion component of the Mohr- Coulomb shear
 364 strength parameters but does not cause orientation of clay particles or a reduction in the friction
 365 angle (Skempton 1970). Because Skempton (1970) concludes that softening over time reduces
 366 clay strength to the “critical state” strength, where further distortion or weathering will not result
 367 in any change in water content, the strength is approximately equal to the strength of the soil

368 when it is normally consolidated. For London clay, the difference between the “critical state”
369 strength (22.5 degrees) and the peak strength of normally consolidated London Clay (20 degrees)
370 is about 2.5 degrees (Skempton, 1970). Thus, Skempton (1970) concludes that equating the
371 strength of normally consolidated test specimens to the fully softened strength is a “somewhat
372 conservative” approximation.

373

374 Because the fully softened shear strength corresponds to the drained peak strength of a
375 normally consolidated specimen, this suggests that the value of effective stress cohesion (c')
376 should be set to zero, i.e., the value of cohesion measured in shear tests on normally consolidated
377 clay (Holtz and Kovacs 1981, Terzaghi et al. 1996), for the analysis of first time slides in
378 overconsolidated clays. This is important because even small values of c' can result in significant
379 differences in calculated factors of safety especially in shallow slides, such as levee or
380 embankment slopes. However, back analysis of first-time slides in London clay, indicate small
381 values of c' , approximately 0.96 kPa (20 psf), can be mobilized (Chandler and Skempton, 1974).
382 Skempton (1977) also suggests a c' of 0.96 kPa (20 psf) and ϕ'_{fs} of 20 degrees for London clay.
383 Mesri and Abdel-Ghaffar (1993) back-analyzed forty-five case histories and conclude c' can
384 range from zero to 24 kPa. In summary, the fully softened value of cohesion should be zero
385 unless back-analysis of local case histories suggests a value greater than zero.

386

387

388 **SPREADSHEET FOR EMPIRICAL CORRELATIONS**

389

390 During the present study a spreadsheet was developed that utilizes only two parameters, CF and
391 LL, as input and generates values of ϕ'_r and ϕ'_{fs} for effective normal stresses of 0, 50, 100, 400,
392 and 700 kPa. The spreadsheet uses the equations for the various trend lines presented herein and
393 is an electronic supplement to this paper. The estimated stress dependent residual and fully
394 softened strength envelopes are plotted on a single figure in the spreadsheet as well as tables of
395 shear stress and effective normal stress for the fully softened and residual strength envelopes.
396 The tabulated values of effective normal stress and shear stress can be used directly in slope
397 stability software to describe the stress dependent strength envelope instead of using values of
398 effective stress cohesion (c') and friction angle (ϕ'). The advantage of showing both drained

399 residual and fully softened strength envelopes on the same graph is the user can compare the
400 difference between the fully softened and residual strengths in a single figure to determine the
401 importance of identifying whether or not a preexisting shear surface is present or will develop in
402 the slope and if so, how much of the failure surface should be assigned a residual strength.

403

404

405 **EFFECT OF SAMPLE PREPARATION ON STRENGTH AND INDEX PROPERTIES**

406

407 **Effect of Sample Preparation on ϕ'_r**

408

409 The drained residual strength is a fundamental property because the soil structure, stress history,
410 particle interference, and diagenetic bonding have been removed by continuous shear
411 displacement in one direction (Stark et al., 2005). As a result, the residual strength is controlled
412 by the frictional resistance of individual clay mineral particles, oriented primarily face-to-face,
413 sliding across one another. The frictional shear resistance induced by sliding of individual clay
414 mineral particles is controlled by the fundamental characteristics of the clay particles, e.g., type
415 of clay mineral(s) and quantity or percentage of the clay mineral(s). Thus, laboratory preparation
416 and shear testing must be able to disaggregate the clay mineral particles so they can be
417 individually oriented parallel to the direction of shear.

418

419 Skempton (1964) suggests field shear movement of about a meter is required to achieve a
420 residual strength condition. This field shearing causes an increase in fines content of the material
421 along the shear surface by pushing silt and sand sized particles away from the shear surface.
422 Mesri and Cepeda-Diaz (1986) conclude “the shearing process itself disaggregates and orients
423 even the clay plates at the surface of aggregates adjacent to the shear plane.” Chandler (1969)
424 measured a higher CF in the shear surface than the overall specimen also indicating
425 disaggregation during shear. Thus during the process of achieving a residual strength condition,
426 aggregated clay mineral particles are disaggregated close to individual clay mineral particle size,
427 which must be duplicated in laboratory testing to achieve a residual strength that is consistent
428 with field conditions.

429

430 A remolded soil sample is preferred to an undisturbed shear surface specimen for
431 laboratory residual shear strength testing because of difficulties in sampling, orienting, and
432 shearing in the direction in which shearing had occurred in the field. However, the use of a
433 remolded specimen results in a larger shear displacement being required in the laboratory to
434 disaggregate the clay mineral particles and achieve a residual strength condition than an
435 undisturbed specimen from the shear surface. The laboratory displacement required to reach a
436 residual strength condition can be reduced by using a disaggregated sample and preshearing the
437 resulting test specimen prior to drained shearing. For highly indurated soils, the disaggregation
438 of clay mineral particles in the laboratory can be facilitated by ball milling or pulverizing by
439 some other means, such as disc milling, rod milling, and/or blending, to process the soil through
440 Number 200 sieve to simulate field disaggregation. Silt and clay sized particles that show no
441 induration/aggregation do not require ball milling because ball milling may change the texture
442 and gradation of such soils.

443

444 In summary, disaggregation of highly indurated materials was used in this study to
445 facilitate measurement of the drained residual strength using remolded samples of
446 overconsolidated clays, mudstones, claystones, and shales in the laboratory and to simulate field
447 disaggregation processes that occurs over many years and large shear displacement. Soils with
448 little or no induration/aggregation were only pulverized using a mortar and pestle after air drying
449 and processed through the Number 40 sieve for ring shear and index property testing. Because
450 values of LL and CF measured on disaggregated samples are in better agreement with true values
451 of ϕ'_r , values of LL and CF measured using ball milled samples were used to develop the
452 empirical correlation in Fig. 2 so values of LL and CF measured using disaggregated samples
453 should be used to estimate values of ϕ'_r from Fig. 2.

454

455

456 **Effect of Sample Preparation on ϕ'_{fs}**

457

458 The use of values of LL and CF measured using disaggregated samples of overconsolidated
459 clays, mudstones, claystones, and shales to develop the ϕ'_{fs} correlation in Fig. 4 is less intuitive
460 than described above for the ϕ'_r correlation. In theory, the fully softened shear strength represents

461 the strength of a soil when the effects of overconsolidation are removed. Thus the strength
462 corresponds to a normally consolidated soil and it reflects the ability of particles to establish
463 short range and random interaction and interlocking (Mesri and Cepeda-Diaz, 1986). The fully
464 softened shear strength is measured at a small shear displacement so significant reorientation of
465 the particles parallel to the direction of shear has not occurred. Thus, particle size and shape do
466 affect the measured value which should be greater than the frictional shear resistance of
467 reoriented particles. It is expected that during mobilization of the fully softened shear strength in
468 the field, the clay particles retain at least some of their natural structure and there is little
469 orientation of clay particles along the shear surface in the direction of shear as happens in
470 achieving a residual strength condition.

471
472 In the field, the clay particles may be close to or completely disaggregated at the fully
473 softened strength condition in highly weathered clays, silts, and compacted clayey fills. If it is
474 desired to simulate full or complete weathering for evaluation of highly weathered clays, silts,
475 and compacted clayey fills, the air-dried soil should be processed through the U.S. Standard
476 Sieve Number 40 and further disaggregated using a blender after soil hydration for at least 48
477 hours. The fully softened strength and index property testing of this material should be
478 performed using the blenderized soil.

479
480 Clay mineral particles may still have some aggregation in indurated, e.g., e.g., claystones,
481 shales, mudstones, materials and in highly plastic, highly overconsolidated clays at the time of
482 sampling even though it is believed a fully softened condition exists. To simulate this level of
483 disaggregation, indurated materials should be processed through the Number 40 sieve and then
484 further disaggregated using a blender after soil hydration for at least 48 hours to reflect a “fully”
485 weathered condition before strength testing as suggested above. However, there is some field
486 evidence that even indurated materials, e.g., claystones, shales, mudstones, may over the life of a
487 project become so weathered that their particles are substantially disaggregated but not
488 reoriented parallel to the direction of shear, i.e., residual strength condition. If full
489 disaggregation of indurated material due to weathering and softening is anticipated or desired for
490 design or analysis purposes, the material could be ball or disc-milled, processed through the

491 Number 200 sieve, hydrated, and then blenderized before fully softened strength and index
492 property testing to reflect a “fully” weathered condition.

493
494 In all preparation procedures, care must be exercised for those materials containing non-
495 clay or silt sized particles to avoid breakdown of these larger particles during processing and
496 changing the gradation of the soil. Whatever sample preparation procedure is used to simulate a
497 “fully” weathered condition, it should be carefully documented so the resulting data can be
498 properly interpreted for design and properly compared to existing fully softened strength
499 correlations such as the one presented herein.

500
501 Empirical correlation for drained fully softened secant friction angles in Fig. 4 was
502 developed using LL and CF values measured using disaggregated samples to make it compatible
503 with the empirical correlation for drained residual secant friction angles and easy comparison by
504 the users. To facilitate use of the empirical correlations, adjustment factors to estimate values of
505 LL and CF measured using disaggregated samples from ASTM derived values of LL and CF are
506 discussed below.

507
508

509 **Effect of Sample Preparation on LL and CF**

510
511 Because the empirical correlations for drained residual and fully softened secant friction angle
512 use index properties measured using disaggregated soil samples for overconsolidated clays,
513 mudstones, claystones, and shales, the effect of sample preparation on index properties is
514 discussed in this section. Non-aggregated materials, e.g., silty clay or clayey, compacted fill,
515 were not ball milled and only processed through Number 40 sieve as required by ASTM D4318
516 and D422 (ASTM, 2010c and 2010d) for measuring LL and CF, respectively.

517
518 Preparation of a remolded specimen can influence the measured LL. For example, La
519 Gatta (1970) shows that disc milling Cucaracha shale from the Panama Canal for six minutes
520 resulted in an increase in LL from 49% to 156%. La Gatta (1970) and Townsend and Banks
521 (1974) suggest that the degree of induration (aggregation) that survives a particular sample

522 preparation procedure will influence the measurement of the index properties. Mesri and Cepeda
523 (1986) conclude that most heavily overconsolidated clays, mudstones, claystones, and shales
524 possess varying degrees of induration. This induration involves diagenetic bonding between clay
525 mineral particles by carbonates, silica, alumina, iron oxides, and other ionic complexes. Mesri
526 and Cepeda (1986) suggest ball milling of highly overconsolidated clay specimens to “free” or
527 disaggregate the clay mineral particles. Ball milling is suggested and only used herein for highly
528 overconsolidated clays, mudstones, claystones, and shales because they possess substantial
529 diagenetic bonding that is usually not destroyed using a mortar and pestle. To measure LL,
530 which is used herein to infer clay mineralogy, the indurated mudstone, claystone, and shale
531 samples are air-dried, disaggregated by ball-milling, and processed through a Number 200 sieve.
532 Disaggregation of highly overconsolidated particles by ball/disc milling, blending/grinding
533 (Townsend and Banks, 1974), or other suitable means, results in a better estimate of the actual
534 LL than ASTM test methods (2010a) because more of the diagenetic bonding and induration is
535 eliminated which allows more particle surface area to be exposed and hydrate than if the clay
536 particles are not disaggregated. Thus, a clay sample with disaggregated particles usually results
537 in a higher LL than that obtained using the ASTM (2010a) test method.

538
539 Normally to lightly overconsolidated fine-grained materials that are not indurated
540 (aggregated), do not require disaggregation of clay mineral particles. As a result, these materials
541 should be processed through Number 40 sieve as suggested by ASTM (2010a) and used for
542 measuring LL and CF. The ball/disc milling of non-indurated clay materials could result in
543 changing the texture and gradation of the soil. Therefore, judgment is required to determine
544 whether or not a material should be ball-milled or not (Stark et al., 2005). This decision can be
545 made after examination of the material and determining whether the materials can be sufficiently
546 broken down with a mortar and pestle to disaggregate the clay particles. If not, ball/disc milling
547 or any other means (blending/grinding) should be used to disaggregate the clay particles so the
548 material can be processed through Number 200 sieve.

549
550 Stark et al. (2005) present a relationship between ball milled derived LL and ASTM
551 derived LL using fourteen soil samples of highly overconsolidated clays. The correlation

552 suggested by Stark et al. (2005) facilitates the estimation of ball milled derived LL values from
553 the ASTM derived LL because ball/disc milling requires special equipment and extra effort that
554 may not be readily available in practice. Because commercial laboratories primarily, if not
555 exclusively, utilize the ASTM (2010a) to measure LL, this correlation can be used to estimate
556 the ball milled derived LL to obtain a representative value of LL for highly indurated materials.

557

558 Test results for fifteen additional soils, i.e., a total 29 soils, were used herein to develop a
559 new relationship between the ASTM derived LL using the Number 40 sieve, referred herein as
560 $LL_{\#40}$, and the LL measured on a sample processed through Number 200 sieve, referred herein as
561 $LL_{\#200}$. The resulting relationship is expressed in Equation (8) and can be used with an ASTM
562 derived value of LL ($LL_{\#40}$) to estimate the $LL_{\#200}$ value for a particular soil. This should reduce
563 the need for commercial laboratories to ball/disc mill overconsolidated clays, claystones, shales,
564 and mudstones and process the material through a Number 200 sieve to estimate representative
565 values of LL and strength envelopes.

566

$$567 \quad \frac{LL_{\#200}}{LL_{\#40}} = 0.003(LL_{\#40}) + 1.23 \quad (8)$$

568

569 Equation (8) shows the ratio of $LL_{\#200}/LL_{\#40}$ increases with increasing $LL_{\#40}$. It is
570 anticipated that the higher the LL, the greater the bonding between clay mineral particles and the
571 more difficult disaggregation of the clay particles becomes, which results in the greatest
572 difference between values of $LL_{\#40}$ and $LL_{\#200}$. Thus, high plasticity claystones, shales, and
573 mudstones should be processed through Number 200 sieve before measuring LL or the LL
574 values adjusted using Equation (8).

575

576 The field conditions under which the residual, and possibly fully softened, strength are
577 mobilized, i.e., disaggregated clay particles, also results in a higher CF. In other words, along a
578 preexisting shear surface the soil particles will be disaggregated so the LL and CF should reflect
579 this field condition. ASTM (2010b) derived CF, called herein $CF_{\#40}$, and CF measured using
580 material processed through Number 200 sieve, called herein $CF_{\#200}$, were used to develop a

581 correlation between these values of CF. Because commercial laboratories primarily utilize
582 ASTM (2010b) to measure CF, Stark et al. (2005) present a relationship between $CF_{\#40}$ and
583 $CF_{\#200}$ measured using samples of fourteen different highly overconsolidated clays. The present
584 study used test results for eighteen additional soils, i.e., a total of 32 soils, to develop the
585 relationship in Equation (9). Equation (9) can be used to estimate the value of $CF_{\#200}$ which may
586 be a more representative of the field value of CF for highly indurated clays.

587

588 Equation (9) shows the $CF_{\#200}/CF_{\#40}$ ratio decreases as $CF_{\#40}$ increases. It is anticipated
589 that this decrease is caused by the $CF_{\#40}$ value being in better agreement with the $CF_{\#200}$ value at
590 higher values of CF. Stark et al. (2005) suggest that this may be attributed to the dispersing
591 agent, sodium hexametaphosphate, being more effective in high plasticity soils than low
592 plasticity soils or processing the material through the Number 40 sieve is sufficient to
593 disaggregate the material because CF is so high.

594

$$595 \quad \frac{CF_{\#200}}{CF_{\#40}} = 0.0002(CF_{\#40})^2 - 0.0278(CF_{\#40}) + 2.15 \quad (9)$$

596

597

598 **SUMMARY AND CONCLUSIONS**

599

600 Updated empirical correlations for drained residual and fully softened secant friction angles
601 using LL, CF, and effective normal stress are presented. For consistency between the empirical
602 correlations for drained residual and fully softened secant friction angles, ϕ'_r and ϕ'_{fs} are plotted
603 against LL and CF measured using soil processed through the Number 200 or coarser sieve for
604 highly indurated clays and shales and processed through the Number 40 sieve for all other soils.

605

606 The trend lines in the new empirical correlations for drained residual and fully softened
607 secant friction angles are modeled using mathematical expressions to facilitate distribution and
608 use in practice. A separate equation is developed for each trend line in each CF group. The
609 mathematical expressions reduce the need to utilize the graphical version of the empirical
610 correlations.

611

612 A spreadsheet developed during the present study incorporates the mathematical
613 expression for each trend line and is submitted as an electronic supplement to this paper. The
614 spreadsheet requires only two input parameters, LL and CF, and generates values of ϕ'_r and ϕ'_{fs}
615 for different effective normal stresses that can be used to develop the stress dependent failure
616 envelopes. The resulting stress dependent residual and fully softened strength envelopes can be
617 used directly in slope stability analyses for preexisting and first-time landslides, respectively, and
618 are compared to assess the importance of identifying the presence or development of a shear
619 surface.

620

621 Sample preparation affects LL and CF values therefore these parameters should be
622 measured using the following procedure:

623

624 • Clay soils with little or no induration (aggregation) should be processed through
625 Number 40 sieve in accordance with relevant ASTM test methods (2010 a and b)
626 for both residual and fully softened strength testing.

627

628 • Highly indurated (aggregated)/heavily overconsolidated clays and shales should be
629 disaggregated by processing the material through the Number 200 sieve using ball
630 milling or some other disaggregation method for residual strength testing and
631 possibly for fully softened strength testing depending on the degree of weathering
632 and softening to be simulated.

633

634 ASTM derived values of LL and CF measured using soil samples processed through
635 Number 40 sieve can be converted to LL and CF values measured using disaggregated soil
636 samples by empirical expressions in Equations (8) and (9) to estimate stress dependent strength
637 envelopes from the correlations presented herein.

638

639

640

641

642 **REFERENCES**

- 643
- 644 ASTM, (2010a). “Standard test method for torsional ring shear test to determine drained residual
645 shear strength of cohesive soils.” (*D6467*), West Conshohocken, Pa.
- 646 ASTM, (2010b). “Standard test method for Torsional Ring Shear Test to Determine Drained
647 Fully Softened Shear Strength and Nonlinear Strength Envelope of Cohesive Soils (Using
648 Normally Consolidated Specimen) for Slopes with No Preexisting Shear Surfaces.”(*D7608*),
649 West Conshohocken, Pa.
- 650 ASTM, (2010c). “Standard test method for liquid limit, plastic limit, and plasticity index of soil.”
651 (*D4318*), West Conshohocken, Pa.
- 652 ASTM, (2010d). “Standard test method for particle-size analysis of soils.” (*D422*), West
653 Conshohocken, Pa.
- 654 Bjerrum, L., (1967). “Progressive failure in slopes of overconsolidated plastic clays.” *Int J. Soil*
655 *Mech. Eng. Div., ASCE, SM5, 1-49.*
- 656 Bjerrum, L. and Simons, N. E. (1960). “Comparison of shear strength characteristics of normally
657 consolidated clays.” *Proc., Conf. on Shear Strength of Cohesive Clays, ASCE, Boulder, CO,*
658 *711-726.*
- 659 Brooker, E. W. and Ireland, H. O., (1965). “Earth pressures at rest related to stress history.” *Can.*
660 *Geotech. J., 2(1), 1-15.*
- 661 Chandler, R. J., (1969). “The effect of weathering on the shear strength properties of Keuper
662 Marl.” *Geotechnique, 19(3), 321-334.*
- 663 Chandler, R. J., (1977). “Back analysis techniques for slope stabilization works: a case record.”
664 *Geotechnique, 27(4), 479-495.*
- 665 Chandler, R. J. and Skempton, A.W. (1974). “The design of permanent cutting slopes in stiff
666 fissured clays.” *Géotechnique, 24(4), 457-466.*
- 667 Collotta, T., Cantoni, R., Pavesi, U., Ruberl, E., and Moretti, P. C. (1989). “A correlation
668 between residual friction angle, gradation and the index properties of cohesive soils.”
669 *Geotechnique, 39(2), 343-346.*

670 Deere, D. U., (1967). "Shale mylonites-their origin and engineering properties." Ass. Eng. Geol.,
671 Nat. Meeting, Dallas, Texas.

672 Eid, H.T. (1996). "Drained shear strength of stiff clays for slope stability analyses." *PhD thesis*,
673 *University of Illinois at Urbana-Champaign, USA*.

674 Eid, H.T. (2006). "Factors influencing determination of shale classification indices and their
675 correlation to mechanical properties." *J. Geotech. and Geol. Eng.*, 24, 1695-1713.

676 Holt, J. K., (1962). "The soils of Hong Kong" s coastal waters." *Symp. Hgng Kong Joint Group*
677 *Committee, Hong Kong: Inst. Civ., Mech. and Elect. Engrs.*, 33-51.

678 Kanji, M. A., (1974). "Relationship between drained friction angles and Atterberg limits of
679 natural soils." *Geotechnique*, 24(4), 671-674.

680 Kenney, T. C., (1967). "The influence of mineral composition on the residual strength of natural
681 soils." *Proc. Geotech. Conf, Oslo*, 1, 123-129.

682 La Gatta, D.P. (1970). "Residual strength of clays and clay-shales by rotation shear tests."
683 *Harvard Soil Mechanics Series No. 86*, Harvard University, Cambridge, Massachusetts.

684 Lupini, J. F., Skinner, A. E., Vaughan, P. R. (1981). "The drained residual strength of cohesive
685 soils." *Geotechnique*, 31(2), 181-213.

686 Mesri, G., and Cepeda-Diaz, A. F., (1986). "Residual shear strength of clays and shales."
687 *Geotechnique*, 36(2), 269-274.

688 Mesri, G., and Abdel-Ghaffar, M. E. M., (1993). "Cohesion intercept in effective stress-stability
689 analysis." *J. Geotech. Geoenviron. Eng.*, 119(8), 1229-1249.

690 Mesri, G., and Shahien, M., (2003). "Residual shear strength mobilized in first-time slope
691 failures." *J. Geotech. Geoenviron. Eng.*, 129(1), 12-31.

692 Mitchell. J. K. (1993). *Fundamentals of Soil Behavior* 2nd Ed., Wiley.New York.

693 Mitchell, N. W. R. (1965). Direct shear tests on thin samples of remolded shales from the
694 Bighorn Mountains, Wyoming. MS thesis, University of Illinois, pp 49.

695 NAVFAC, (1971). “Design Manual: Soil Mechanics, Foundations, and Earth Structures,
696 NAVFAC, DM-7.” Department of the Navy, Naval Facilities Engineering Command,
697 Alexandria, VA.

698 Seycek, J., (1978). “Residual shear strength of soils.” *Bull. Intl. Assoc. Engrg. Geol.*, Vol. 17,
699 73-75.

700 Skempton, A. W., (1964). “Long term stability of clay slopes.” Fourth Rankine Lecture,
701 *Geotechnique*, 14(2), 77-101.

702 Skempton, A. W., (1970). “First time slides in overconsolidated clays.” *Geotechnique*, 20(3),
703 320-324.

704 Skempton, A. W., (1977). “Slope Stability of cuttings in brown London clay.” *Proceedings of*
705 *9th International Conference of Soil Mechanics and Foundations*, Tokyo, Vol. 3, 261-270.

706 Skempton, A. W., (1985). “Residual strength of clays in landslides, folded strata and the
707 laboratory.” *Geotechnique*, 35(1), 3–18.

708 Stark, T. D., and Eid, H. T., (1994). “Drained residual strength of cohesive soils.” *J. Geotech.*
709 *Geoenviron. Eng.*, 120(5), 856-871.

710 Stark, T. D., and Eid, H. T., (1997). “Slope stability analyses in stiff fissured clays.” *J. Geotech.*
711 *Geoenviron. Eng.*, 123(4), 335–343.

712 Stark, T. D., Choi, H., and McCone, S., (2005). “Drained shear strength parameters for analysis
713 of landslides.” *J. Geotech. Geoenviron. Eng.* 131(5), 575-588.

714 Terzaghi, K. (1936). “Stability of slopes of natural clay.” *Proceedings of the 1st International*
715 *Conference of Soil Mechanics and Foundations*, 161-165.

716 Terzaghi, K., Peck, R. B., and Mesri, G. (1996). *Soil Mechanics in Engineering Practice*, 3rd Ed.
717 Wiley. New York, 549-549.

718 Tiwari, B., and Marui, H., (2005). “A New Method for the Correlation of Residual Shear
719 Strength of the Soil with Mineralogical Composition.” *J. Geotech. Geoenviron. Eng.*, 131(9),
720 1139–1150.

721 Townsend, F. C., and Gilbert, P. A. (1974). "Preparation effects on clay shale classification
722 indexes." *Proc., Nat. Meeting on Water Resources Eng.*, ASCE Los Angeles, CA, Jan 21-25,
723 1-30.

724 Voight, B. (1973)., "Correlation between Atterberg plasticity limits and residual shear strength of
725 natural soils." *Geotechnique*, 23(2), 265-267.

726 Wesley, L.D. (2003). "Residual strength of clays and correlations using Atterberg limits."
727 *Geotechnique*, 53(7), 669-672.

728 Wright, S. G., Zornberg, J. G., and Aguetant, J. E. (2007). "The Fully Softened Shear Strength
729 of High Plasticity clays." Center for Transportation Research, University of Texas at Austin.
730

731
732
733
734
735
736
737
738
739
740
741
742
743
744
745
746
747
748
749
750
751

FIGURE CAPTIONS:

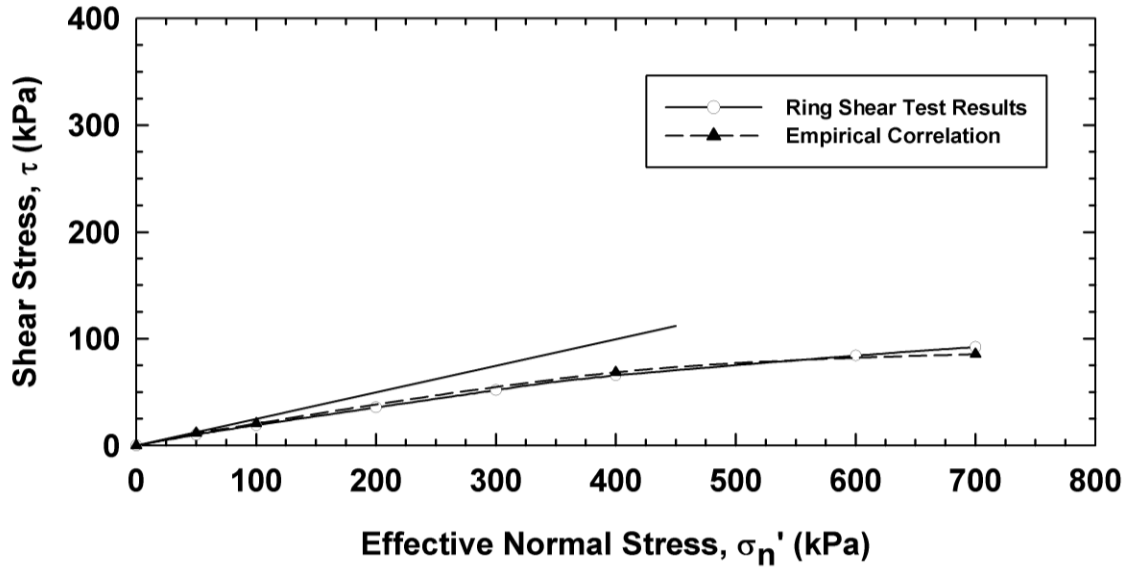
Fig. 1. Stress dependent drained residual strength envelope from ring shear test results and empirical correlation from Stark et al. (2005)

Fig. 2. Updated empirical correlation for drained residual secant friction angle based on liquid limit (LL), clay-size fraction (CF), and effective normal stress (σ'_n) for seventy-three natural soils

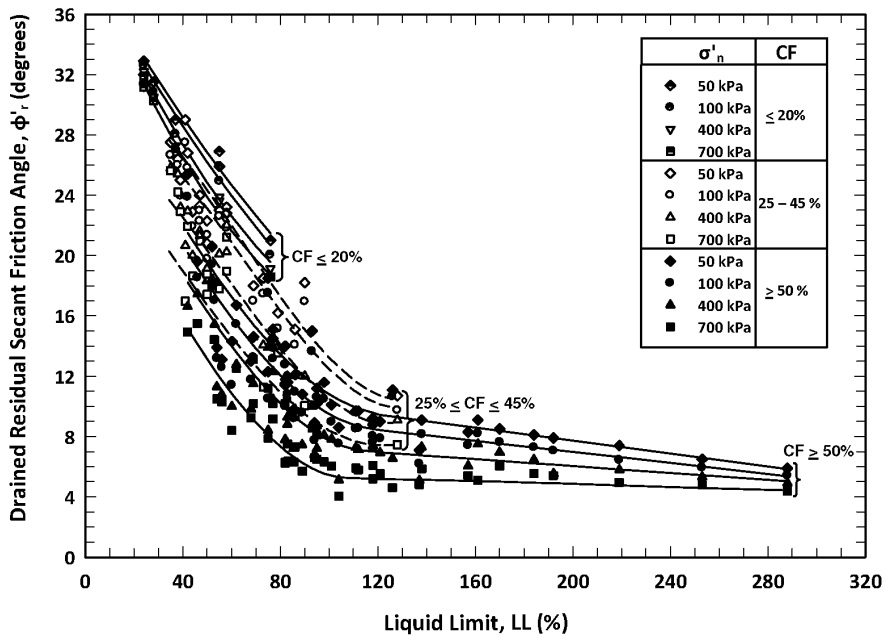
Fig. 3. Comparison of drained residual secant friction angle trend line suggested by Stark et al. (2005) and those estimated using Equations (1.1) to (1.4) for CF Group #1 (CF<20%)

Fig. 4. Updated empirical correlation for drained fully softened secant friction angle based on liquid limit (LL), clay-size fraction (CF), and effective normal stress (σ'_n) for thirty-nine natural soils

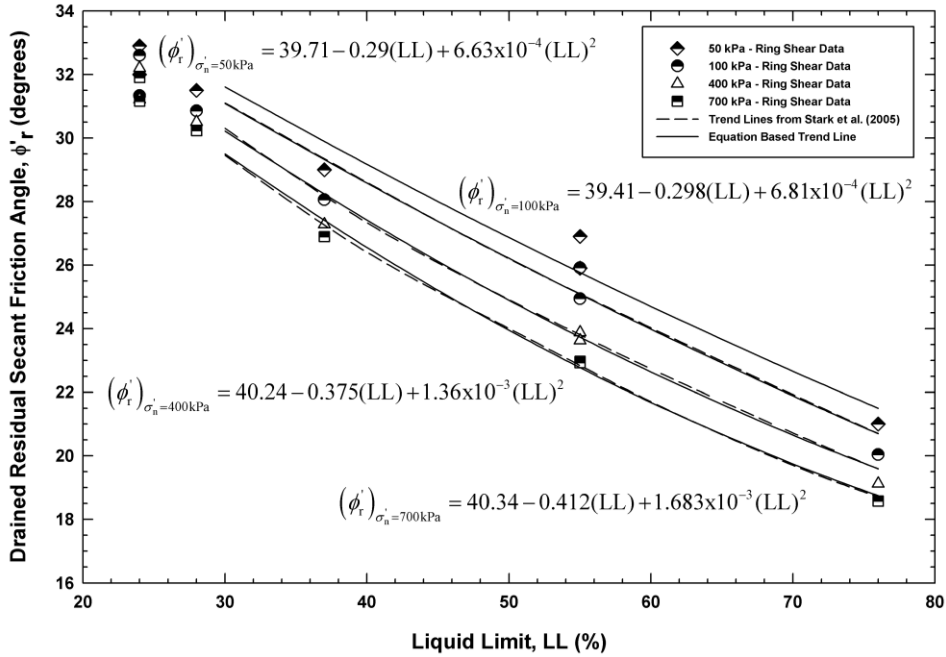
Fig. 5. Comparison of drained fully softened secant friction angle trend lines suggested by Stark et al. (2005) and those estimated using mathematical Equations (7.1) to (7.3) for CF Group #3 ($25\% \leq CF \leq 45\%$).



752
 753 **Fig. 1.** Stress dependent drained residual strength envelope from ring shear test results and
 754 empirical correlation from Stark et al. (2005)
 755

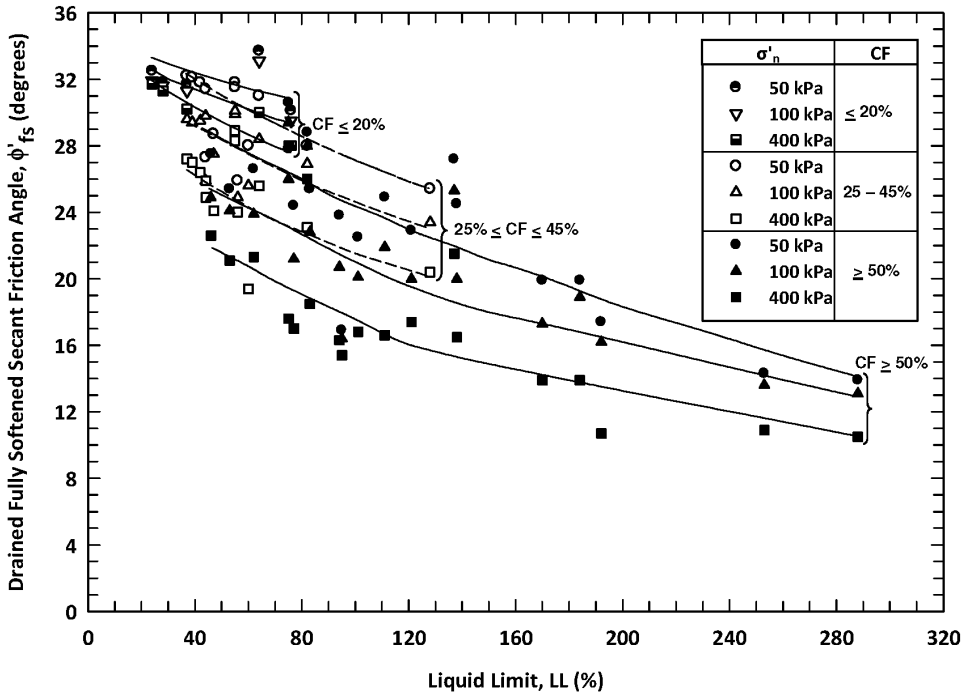


756
 757 **Fig. 2.** Updated empirical correlation for drained residual secant friction angle based on liquid
 758 limit (LL), clay-size fraction (CF), and effective normal stress (σ'_n) for seventy-three
 759 natural soils
 760



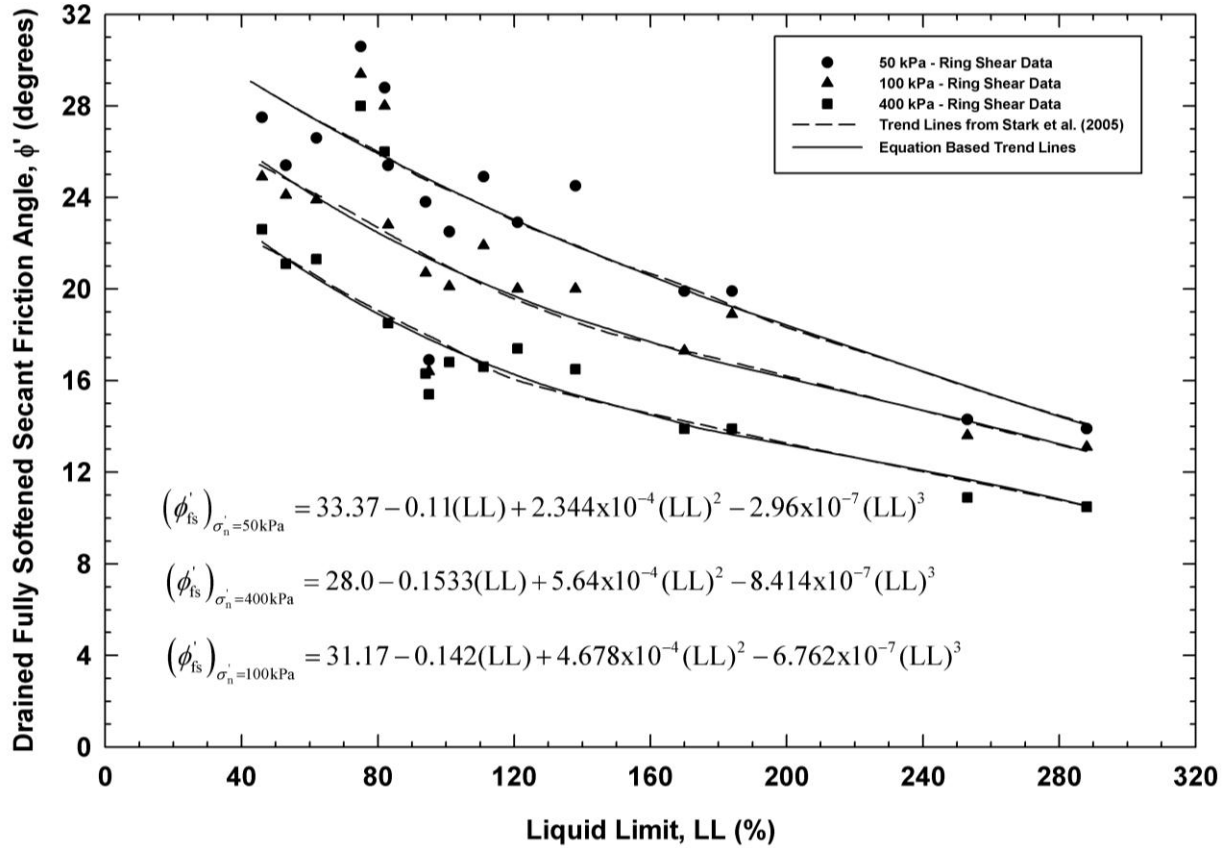
761
762
763
764

Fig. 3. Comparison of drained residual secant friction angle trend line suggested by Stark et al. (2005) and those estimated using Equations (1.1) to (1.4) for CF Group #1 (CF < 20%)



765
766
767
768

Fig. 4. Updated empirical correlation for drained fully softened secant friction angle based on liquid limit (LL), clay-size fraction (CF), and effective normal stress (σ'_n) for thirty-nine natural soils



770
 771
 772
 773
 774
 775

Fig. 5. Comparison of drained fully softened secant friction angle trend lines suggested by Stark et al. (2005) and those estimated using mathematical Equations (7.1) to (7.3) for CF Group #3 ($25\% \leq CF \leq 45\%$).